MESENCHYMAL STEM CELL SECRETOME DECREASES THE INFLAMMATORY RESPONSE IN ANNULUS FIBROSUS ORGAN CULTURES

C. Neidlinger-Wilke[1,§], A. Ekkerlein[1,§], R.M. Goncalves[1,2,3,4], J.R. Ferreira[2,3,4], A. Ignatius[1], H.J. Wilke[1] and G.Q. Teixeira[1,*]

[1] Institute of Orthopaedic Research and Biomechanics, Trauma Research Centre, Ulm University, Ulm, Germany
[2] Instituto de Investigação e Inovação em Saúde (i3S), Universidade do Porto, Porto, Portugal
[3] Instituto de Engenharia Biomédica (INEB), Universidade do Porto, Porto, Portugal
[4] Instituto de Ciências Biomédicas Abel Salazar (ICBAS), Universidade do Porto, Porto, Portugal
[§] These authors contributed equally to this work

Abstract

Mesenchymal stem/stromal cell (MSC)-based therapies have been proposed for back pain and disc degeneration, despite limited knowledge on their mechanism of action. The impact of MSCs/their secretome on annulus fibrosus (AF) cells and tissue was analysed in bovine AF organ cultures (AF-OCs) exposed to upper-physiological cyclic tensile strain (CTS, 9 %, 1 Hz, 3 h/d) and interleukin (IL)-1β in a custom-made device. A 4 d treatment of the CTS + IL-1β-stimulated AF-OCs with MSC secretome downregulated the expression of inflammation markers [*IL-6*, *IL-8*, prostaglandin-endoperoxide synthase 2 (*PTGS2*)], complement system regulators [cluster of differentiation (*CD*)*46*, *CD55*, *CD59*] and matrix metalloproteinase 1 but also of tissue inhibitors of metalloproteinases (*TIMP-1*, *TIMP-2*) and collagen type I. At the protein level, it was confirmed that IL-6, MMP-3 and collagen content was decreased in AF-OCs treated with the MSC secretome compared to the CTS + IL-1β stimulation alone. 9 d after treatment, a biomechanical peel-force test showed that the annular adhesive strength was significantly decreased by the MSC secretome treatment. Overall, MSC secretome had a stronger impact on AF tissue than MSCs in co-culture. The secretome contributed to a decrease in the inflammatory and catabolic status of AF cells activated by CTS + IL-1β and played a role in the regulation of the complement system. However, it also contributed to a decrease in collagen at the gene/protein level and in AF mechanical strength compared to the CTS + IL-1β stimulation alone. Therefore, the use of MSC secretome requires further investigation regarding its influence on disc matrix properties.

Keywords: Intervertebral disc, degeneration, herniation, repair/regeneration, mechanical loading, inflammation, complement, paracrine signalling.

***Address for correspondence**: Dr Graciosa Quelhas Teixeira, Institute of Orthopaedic Research and Biomechanics, Trauma Research Centre, Ulm University, Helmholtzstraße 14, 89081 Ulm, Germany. Telephone number: +49 73150055324   Email: graciosa.teixeira@uni-ulm.de

List of Abbreviations			
		COL1A1	collagen type I alpha 1 chain
		COL2	collagen type II
b	bovine gene	COX-2	cyclooxygenase-2
h	human gene	CTS	cyclic tensile strain
ACAN	aggrecan	DMEM	Dulbecco's modified Eagle medium
ADAMTS	a disintegrin and metalloproteinase with thrombospondin motifs	ELISA	enzyme-linked immunosorbent assay
AF	annulus fibrosus	GAPDH	glyceraldehyde 3-phosphate dehydrogenase
AF-OC	AF organ culture		
CCL	chemokine (C-C motif) ligand 2	IL	interleukin
CD	cluster of differentiation	IL-1ra	IL-1 receptor antagonist
CFH	complement factor H	IVD	intervertebral disc

LM   lamella matrix
NOS2   nitric oxide synthase 2
MMP   matrix metalloproteinase
MSC   mesenchymal stem/stromal cells
NP   nucleus pulposus
PGE_2 prostaglandin E_2
PTGS2   prostaglandin-endoperoxide
            synthase 2
sGAG   sulphated glycosaminoglycan
TCC   terminal complement complex
TIMP   tissue inhibitors of MMPs
TLBN   translamellar bridging network
VEGF   vascular endothelial growth factor

Introduction

IVD degeneration and related inflammation are frequently associated with back, neck and radicular pain, major causes of disability globally representing a significant economic burden (Moradi-Lakeh *et al.*, 2017; Murray *et al.*, 2015). Current treatments ranging from physiotherapy to invasive surgeries, including spine fusion and IVD replacement, may decrease the symptoms' progression but fail to restore the native IVD properties. Therefore, there is an urgent need to develop therapies supporting IVD regeneration.

While IVD degeneration is normally associated with ageing (Roberts *et al.*, 2006), cases of early degeneration are also frequently observed. The degenerative IVD pathogenesis may be caused by genetic predisposition, injury and/or lifestyle among others. Disc degeneration involves the interplay between several mechanisms, including mechanical overloading, catabolic cell response, degradation of matrix proteoglycans and loss of water-binding capacity (Adams and Roughley, 2006; Vergroesen *et al.*, 2015), as well as cell senescence and apoptosis (Roberts *et al.*, 2006). These events are frequently associated with an immune response, which plays an important role in the pathogenesis of IVD degeneration and cell death. During these events, the production of extracellular-matrix-degrading enzymes (MMP-1, -3, -13, ADAMTS-4, -5, -13, *etc.*), proinflammatory mediators (IL-1β, -6, -8, tumour necrosis factor-α, *etc.*) and chemoattractants of immune cells (CCL2, CCL5) has been identified (Molinos *et al.*, 2015; Risbud and Shapiro, 2014). Complement-mediated processes are known coordinators of several events during inflammation and significantly contribute to inflammation-mediated tissue damage (Ricklin and Lambris, 2013). Upon activation, complement proteins function as chemotactic factors and amplifiers of the inflammatory response (Ricklin and Lambris, 2013). The activation of TCC formation – a complement system activation product that acts as an inflammatory trigger and induces cell lysis – was shown to be abnormally high in human osteoarthritic joints (Wang *et al.*, 2011) and degenerated IVDs, with a predominance in AF cells (Grönblad *et al.*, 2003). However, little is known about complement system

regulation by IVD cells through the production of soluble CFH or the expression of membrane-bound regulators, including membrane cofactor protein (CD46), complement decay-accelerating factor (CD55) and protectin (CD59), which inhibits TCC formation and confers protection from complement-mediated lysis (Noris and Remuzzi, 2013).

The AF consists of concentric lamellae of regularly arranged collagen fibres, which are interconnected by a network of elastin and fibrillin (Yu *et al.*, 2015). The pathomechanism leading to reduced mechanical function is under-investigated; however, the progressive structural weakening of the IVD may contribute to AF failure and tissue herniation (Adams and Roughley, 2006). There is pertinent clinical relevance for a cost-effective, minimally invasive therapeutic approaches to modulate the immune response and ultimately delay or reverse degeneration before AF tear. In recent years, gene-, cell- or molecular-based therapies have been proposed for patients with painful IVDs at early stages of degeneration (Pfirrmann grades III-IV).

Despite the limited regenerative potential of the degenerated AF, it has been hypothesised to benefit from the presence of cells capable of proliferating and differentiating into AF-like cells. Although progenitor cells have been found in the human IVD, their number decreases very rapidly after birth (Sakai *et al.*, 2012), limiting the IVD´s potential to counteract degeneration or recover from an injury. Therefore, cell-based therapies to stimulate IVD regeneration, namely those using bone-marrow-derived MSC, are being increasingly pursued. MSC transplantation potential has been shown to be associated with their ability to differentiate into IVD-like cells, producing IVD matrix components or promoting the stimulation of endogenous IVD cells, thus enabling anti-catabolic and anti-inflammatory effects, as reviewed by Sakai and Anderson (2015). Patients have reported reduced pain in clinical trials after MSC transplantation; however, either no changes in disc morphology or water-binding capacity or only a minor Pfirrmann grading improvement were observed (Noriega *et al.*, 2017; Orozco *et al.*, 2011; Yoshikawa *et al.*, 2010). MSCs secrete anti-inflammatory factors and influence matrix turnover in short-term osteoarthritic synovium and cartilage explant cultures (van Buul *et al.*, 2012). Pereira *et al.* (2016) showed that MSCs seeded on cartilaginous endplates significantly increase the production of growth factors, as well as of COL2 and ACAN in the NP. Cunha *et al.* (2017) observed in a rat disc herniation model less degeneration/herniation in the MSC-transplanted group. Although no significant changes were detected in the extracellular matrix composition, the transplanted MSCs appeared to modulate the immune response towards tissue regeneration (Cunha *et al.*, 2017). A previous study showed that MSCs in co-culture with a proinflammatory/degenerative NP organ culture can modulate the proinflammatory profile of the NP cells, while themselves displaying a proinflammatory

profile (Teixeira *et al.*, 2018). However, because very few MSCs have been found in the IVD tissue, the authors hypothesised that their paracrine effect *via* the secretome might have a larger effect on IVD cells than direct contact. MSCs secrete numerous soluble factors in response to microenvironmental cues, regulating several mechanisms in neighbouring tissues *via* paracrine signalling (Brisby *et al.*, 2013). Accordingly, several studies have suggested the use of MSC secretome for cardiac tissue repair (Dai *et al.*, 2007) and the recovery of hepatic (Parekkadan *et al.*, 2007) and kidney (van Koppen *et al.*, 2012) functions, among others. Moreover, MSC secretome was suggested to stimulate IVD progenitor cell activity *ex vivo* in degenerated human IVD tissue samples towards the repair process (Brisby *et al.*, 2013).

Preconditioning (or priming) of MSCs *ex vivo* by a low oxygen atmosphere and inflammatory stimulus, including IL-1β (Fan *et al.*, 2012), among others, prior to their use in therapy is recognised as an adaptive strategy that tunes the cells to survive in harsh microenvironments and enhances their regulatory control of the innate and adaptive immune responses (Ferreira *et al.*, 2018; Saparov *et al.*, 2016). MSC-mediated immunomodulation has mainly been attributed to paracrine mechanisms associated with the secretion of proinflammatory/immunoregulatory mediators (Krampera *et al.*, 2006; Ren *et al.*, 2008). Nonetheless, the presence of different concentrations of proinflammatory molecules may differently influence their immunomodulatory response (Li *et al.*, 2012), suggesting that their secretome may lead to a more reproducible outcome.

The aims of the present study were to investigate the anti-inflammatory and regenerative effects of i) MSC application or ii) MSC secretome application on a proinflammatory AF-OC model. In this context, the following hypotheses were investigated: i) the proinflammatory environment led to complement system activation and changes in the AF cell phenotype; ii) MSC secretome was more effective in comparison to MSC transplantation to induce immune-mediated changes of AF tissue integrity.

Materials and Methods

MSC expansion and secretome production
Normal bone-marrow-derived MSCs (PT-2501, Lonza) were isolated from bilateral punctures of the posterior iliac crests of human donors (*n* = 3, one female/two males, mean age = 23.3 years). Donor information is summarised in Table 3. MSCs were seeded at a density of 3,000 cells/cm^2 and routinely expanded in MSC medium composed of low-glucose DMEM (21885-108, Gibco) supplemented with 10 % HyClone calf serum (SH30073.03, GE Healthcare), 1 % penicillin-streptomycin (10,000 U/mL penicillin and 10,000 μg/mL streptomycin, 15140-122, Gibco) and 0.5 % amphotericin B (250 μg/mL, 15290-026, Gibco) at 37 °C under a humidified atmosphere

with 8.5 % CO_2. The medium was exchanged twice a week and cells were trypsinised when reaching 70 % confluency.

For the secretome production, 10^6 MSCs were seeded in 6-well plates (657160, Greiner) and incubated for 2 d in 5 mL MSC medium supplemented with 10 ng/mL recombinant human IL-1β (201-LB, R&D Systems) at 37 °C in a humidified atmosphere containing 6 % O_2 and 8.5 % CO_2 (Fig. 1**a**). Subsequently, the secretome was collected and centrifuged at 1,800 ×*g* for 5 min at 4 °C to remove cell debris and then stored at − 80 °C until further use. Cells maintained under basal conditions were also collected for gene expression analysis prior to co-culture with AF-OCs. MSCs in passages 4-9 were used for the experiments.

Tissue dissection and organ culture preparation
AF-OCs were prepared according to Saggese *et al.* (2019). Bovine tails from 12-24-month-old animals (*n* = 20) were obtained from a local slaughterhouse (Fleischmarkt Donautal, Ulm, Germany) and dissected within 2 h after euthanasia. Coccygeal segments 2-3 to 7-8 were isolated and the NP was removed using 14-16 mm diameter punches, depending on the IVD size. The collected AF rings were incubated at 37 °C in a humidified atmosphere of 6 % O_2 and 8.5 % CO_2 in IVD medium composed of low-glucose DMEM supplemented with 5 % FBS Superior (S0615, Biochrom), 1 % non-essential amino acids (11140-035, Gibco), 1 % penicillin-streptomycin, 0.5 % amphotericin B and 1.5 % 5 mol/L NaCl/0.4 mol/L KCl solution to adjust the osmolarity to 400 mOsm, as previously described (Neidlinger-Wilke *et al.*, 2012; Teixeira *et al.*, 2016). The rings were left for 6 d in six-well plates with membrane filter inserts (MCEP06H48, Millipore) and 0.46 MPa static loading (Teixeira *et al.*, 2016). The medium was exchanged every second day.

Treatment of AF rings with MSCs and MSC secretome
On day 6, the AF-OCs were transferred to silicone dishes and placed in a CTS device, as previously established (Saggese *et al.*, 2019). The experimental timeline and groups are depicted in Fig. 1**b**.

For the AF-OCs treated with MSC co-culture, 10^6 MSCs were seeded on top of the AF rings in the CTS device and left for 24 h to adhere. MSCs were expanded as described above in the "MSC expansion and secretome production" section but not pre-conditioned with inflammation factors. On the next day, the medium was exchanged in all experimental groups according to Table 1. AF-OCs were stimulated with CTS at 1 Hz, 3 h/d. The CTS generated a 9 ± 3 % tensile stress of the AF-OC rings, representing a high physiological loading (Saggese *et al.*, 2019). One group was stimulated with CTS + IL-1β alone, while an additional group was stimulated with CTS + IL-1β and MSCs were co-cultured on top of the AF rings. A third group was stimulated with CTS + IL-1β and

the culture medium was mixed with 5 mL MSC secretome produced by 0.2×10^6 MSCs/mL. The MSC secretome was mixed in a 1 : 1 ratio with IVD medium (5 mL MSC secretome + 5 mL IVD medium) supplemented with 10 ng/mL IL-1β. Unstimulated AF rings were defined as the control group.

At day 11, samples were collected for different analyses. The AF rings were separated into three sections: the tissue was either i) immediately shock-frozen in RNAlater ICE (AM7030, Invitrogen) and liquid nitrogen and stored at − 80 °C for RNA isolation, ii) weighed (tissues with weight between 70 and 130 mg were collected) and frozen at − 20 °C for DNA and protein quantification or iii) used for metabolic activity quantification and subsequently fixed in 4 % phosphate-buffered formalin solution (pH 7.4) for immunohistochemical staining.

For the AF-OCs that underwent treatment for 9 d, 50 % of the medium was exchanged at day 11 according to Table 1. At day 16, the AF rings were collected for metabolic activity quantification and mechanical testing. The supernatants were collected for protein quantification.

Metabolic activity of AF cells in organ culture
The metabolic activity of AF cells was assessed using the resazurin reduction assay. AF tissue sections of 70-130 mg wet weight were incubated with 0.02 mg/mL resazurin sodium salt (R7017, Sigma-Aldrich) solution in IVD medium for 2 h at 37 °C. Fluorescence intensity was determined using a spectrophotometer microplate reader (Spark, Tecan), with 530 nm excitation filters and 590 nm emission filters. Results were normalised to the wet weight (mg) for each
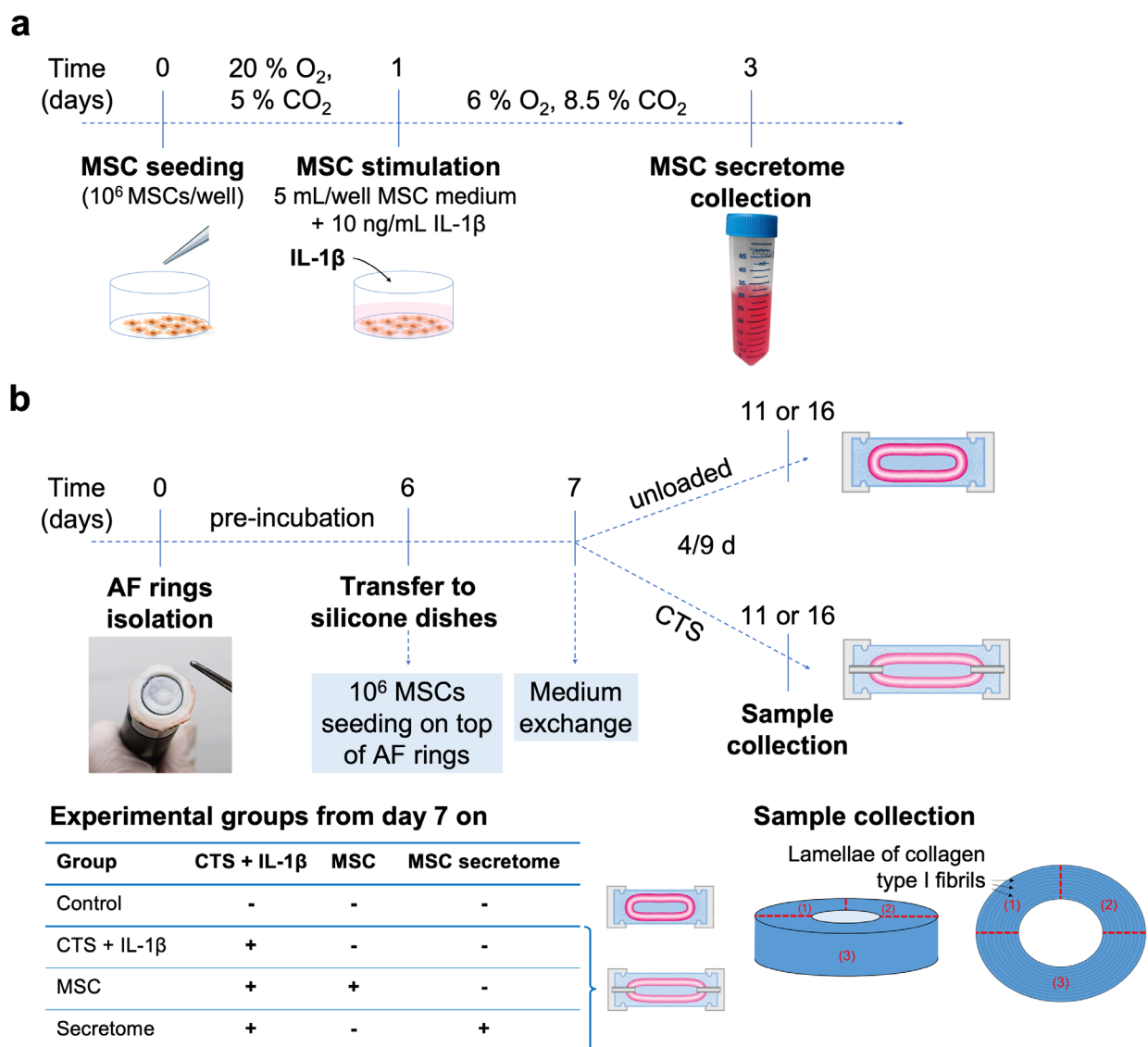

Fig. 1. Experimental timeline and experimental groups. (**a**) MSC secretome was produced by 10^6 MSCs preconditioned with 10 ng/mL IL-1β medium supplementation and culture at 37 °C under 6 % O_2 and 8.5 % CO_2 for 48 h (5 mL/well in 6-well culture plates). (**b**) The AF rings were cultured in a custom-made electromechanical device for the application of CTS to deformable silicone dishes and with IL-1β in the culture medium. The stimulated AF-OCs were either treated with MSCs in co-culture or MSC secretome.

Table 1. Media added at days 7 and 11 of culture to the different experimental groups.

Group	Medium
Control	IVD medium
CTS + IL-1β	IVD medium + 10 ng/mL IL-1β
MSC	IVD medium + 10 ng/mL IL-1β
Secretome	IVD medium + MSC secretome (1 : 1 ratio) + 10 ng/mL IL-1β

Table 2. Bovine oligonucleotide primers used for qRT-PCR. Primers with shown sequence were custom designed; primers with assay ID number were purchased from Applied Biosystems. fw: forward; rev: reverse; b: bovine.

Gene	Sequence (forward and reverse primer)	Product size (bp)
bACAN	fw: 5'-ACA GCG CCT ACC AAG ACA AG-3' rev: 5'-ACG ATG CCT TTT ACC ACG AC- 3'	155
bADAMTS-4	fw: 5'-GAA GCA ATG CAC TGG TCT GA-3' rev: 5'-CTA GGA GAC AGT GCC CGA AG-3'	155
bCD46	assay ID: Bt03224806_m1	97
bCD55	assay ID: Bt03220649_m1	67
bCD59	assay ID: Bt03229098_m1	135
bCOL1A1	assay ID: Bt01463861_g1	61
bGAPDH	fw: 5'-ACC CAG AAG ACT GTG GAT GG-3' rev: 5'-CAA CAG ACA CGT TGG GAG TG-3'	178
bIL-6	fw: 5'-ACC CCA GGC AGA CTA CTT CT-3' rev: 5'-GCA TCC GTC CTT TTC CTC CA-3'	183
bIL-8	fw: 5'-ATT CCA CAC CTT TCC ACC CC-3' rev: 5'-ACA ACC TTC TGC ACC CAC TT-3'	148
bMMP-1	fw: 5'-ATG CTG TTT TCC AGA AAG GTG G-3' rev: 5'-TCA GGA AAC ACC TTC CAC AGA C-3'	193
bMMP-3	assay ID: Bt04259490_m1	76
bNOS2	assay ID: Bt03249602_g1	56
bPTGS2	assay ID: Bt03214492_m1	87
bTIMP-1	assay ID: Bt03223721_m1	57
bTIMP-2	assay ID: Bt03231007_m1	88
bVEGF	fw: 5'-TTG CCT TGC TGC TCT ACC TT-3' rev: 5'-ACA CAG GAC GGC TTG AAA AT-3'	196

Table 3. Human MSC donor information.

MSC donor	Age (years old)	Gender
1	25	female
2	23	male
3	22	male

AF tissue. The AF tissues were frozen at − 20 °C for protein quantification.

Gene expression analysis of AF cells

Tissues frozen in RNAlater ICE were thawed, RNAlater was removed and 1 mL TRIzol was added to the tissue to maintain the RNA integrity during tissue homogenisation performed using a dismembrator (D-9, Miccra GmbH, Heitersheim, Germany). Subsequently, 200 μL of chloroform were added to perform a two-phase extraction of the RNA. Following a 5 min incubation step, the mixture was centrifuged for 30 min at 14,000 ×*g* and 4 °C. RNA was collected and transferred to an RNAse-free reaction tube. By adding an equivalent volume of 70 % EtOH, the RNA was precipitated. RNA isolation was performed using the PicoPure RNA Isolation kit (KIT0204, Thermo Fisher Scientific). For cDNA synthesis with integrated removal of DNA contamination, 12 μL RNA were treated using the QuantiTect Reverse Transcription kit (205313, Qiagen). Gene expression analysis was performed using primers for the reference gene *bGAPDH*, as well as for the target genes (Table 2). The transcribed cDNA

was either mixed with custom-designed primers and Platinum SYBR Green qPCR SuperMix-UDG kit (11733-038, Invitrogen) or TaqMan Gene Expression Assays and Fast Advanced Master Mix (4444557, Applied Biosystems). Runs were performed using the QuantStudio 3 real-time PCR system (Applied Biosystems). Melting curves were analysed to confirm the specificity of the reaction and the quantification cycle 35 was used as cut-off. Relative expression levels were calculated by the Livak method (using the $2^{-\Delta\Delta Ct}$ method), being $\Delta\Delta Ct = \Delta Ct_{(sample\ of\ interest)} - \Delta Ct_{(control\ sample)}$, where $\Delta Ct = Ct_{(gene\ of\ interest)} - Ct_{(GAPDH)}$ (Livak and Schmittgen, 2001).

Protein quantification in the organ culture supernatants

The concentration of PGE_2 (K051-H5, Arbor Assays, Ann Arbor, MI, USA), bIL-6 (MBS9141101, MyBioSource San Diego, CA, USA), hIL-6 (430507, BioLegend), hIL-1β (DLB50, R&D Systems), hIL-1ra (BRA00B, R&D Systems), hCFH (ab137975, Abcam), hTIMP-1 (ELH-TIMP1, RayBiotech, Peachtree Corners, GA, USA) and hTIMP-2 (ELH-TIMP2, RayBiotech) was determined by ELISA in the supernatants at days 11 and 16 of organ culture.

DNA and protein quantification in the AF tissue

AF tissues were digested overnight at 56 °C using 0.5 mg/mL proteinase K (P6556, Sigma-Aldrich) solution for DNA and sGAG quantification. DNA content was determined using the Quant-iT PicoGreen dsDNA assay kit (P7589, Invitrogen). sGAG content was determined using the Blyscan assay kit (B1000, Biocolor, Carrickfergus, UK). AF tissues were digested for soluble collagen and elastin quantification according to the Sircol (S1000, Biocolor) and Fastin (F2000, Biocolor) assay kits, respectively.

Immunohistochemistry

Following fixation in formalin for 48 h, AF samples were washed under running tap water for 2 h, dehydrated and embedded in paraffin-wax. Cross-sections with 7 μm thickness were dewaxed and rehydrated. For antigen retrieval, the sections were incubated with 10 mmol/L citrate buffer (pH 6.0, 85 °C, 20 min), followed by hyaluronidase (2 mg/mL in citrate buffer, pH 8.0, 30 min, 37 °C) and collagenase (2 mg/mL in citrate buffer, pH 8.0, 15 min, 37 °C) digestion. The avidin-biotin complex kit (PK-6100, Vector laboratories) and Vector® NovaRED® Substrate Kit, Peroxidase (HRP) (SK-4800, Vector Laboratories) were used for the immunostaining. Sections were incubated with rabbit anti-IL-6 (1 : 200, bs0782R, Bioss, Woburn, MA, USA) or rabbit anti-MMP3 (1 : 200, ab15191, Abcam) antibodies overnight at 4 °C, according to Saggese *et al.* (2019). Goat anti-rabbit IgG Biotin-XX (1 : 200, B-2770, Invitrogen) was used as secondary antibody. Primary antibodies were polyclonal and reacted with human and bovine molecules. All samples from the same experiment were stained at the same time for each marker for comparison purposes.

Microscopy and image analysis

From each of the IL-6- and MMP-3-stained sections, images were obtained from three different areas. For each area, images were acquired by bright-field and polarised-light microscopy. Polarised-light images were used to distinguish the birefringent LM from the black TLBN regions. To evaluate each staining, the bright-field images were processed using ImageJ software and the colour deconvolution function to separate the Vector® NovaRED® and haematoxylin colour components. Subsequently, the TLBN and the LM were outlined in the Vector® NovaRED® colour channel as regions of interest and the mean pixel intensity was measured for each region. The TLBN/LM ratio of the colour intensities was calculated and the mean of the three images was used to normalise the values of each sample to the control sample from the same experiment. For each experiment ($n = 7$-10) all samples were stained at the same time.

Mechanical testing

A peel test was performed to determine the peeling strength of the AF, according to Gregory *et al.* (2012). AF segments were incised along a central lamella by 5 mm into a "Y" configuration. The split ends of the specimens were fixed in a "T" configuration in a uniaxial material testing machine (Z10, Zwick). The adjacent lamellae were pulled apart at 0.5 mm/s until the complete separation of the tissue. The mean force in the plateau regions of each force-displacement curve was normalised to the height of the AF tissue and used to calculate the delamination strength (Gregory *et al.*, 2012; Saggese *et al.*, 2019)

Statistical analysis

Results are presented as median ± interquartile range. Statistical analysis was performed using GraphPad Prism 8 software (GraphPad Software, Inc.). Data were tested for normal distribution using D'Agostino-Pearson omnibus normality test. Parametric data were analysed using unpaired *t*-test to determine differences between two groups or one-way analysis of variance to determine differences between three or more groups. Nonparametric data were analysed using Kruskal-Wallis test with Dunn's multiple comparison test to determine differences between three or more groups. Significance was set at $p < 0.05$.

Results

Analysis of cell viability and gene expression profile of AF cells

To induce a degenerative and proinflammatory environment, AF-OCs were stimulated day 7 after isolation with CTS + IL-1β. The rings were either
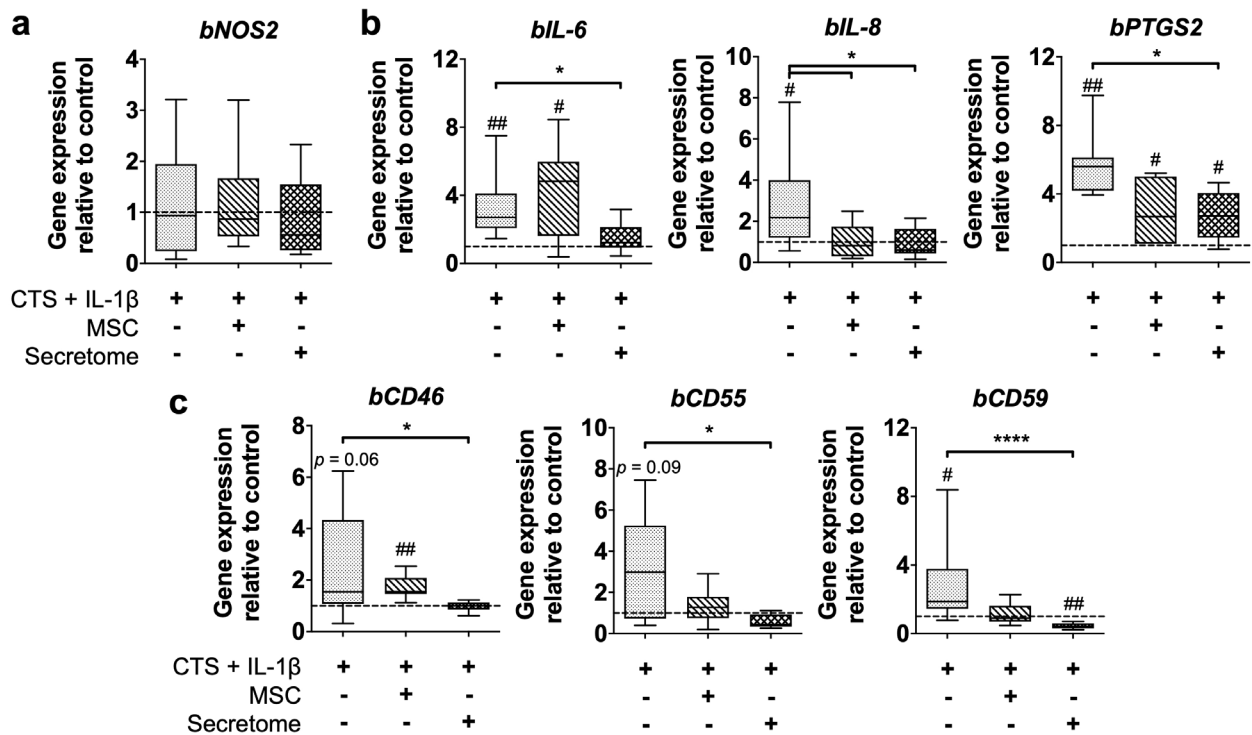
Fig. 2. Gene expression of bovine AF cells at day 11 of organ culture. (**a**) Relative mRNA expression of bovine cell survival marker *bNOS2*, (**b**) proinflammatory markers and (**c**) complement regulators. Results were normalised to the expression level of *bGAPDH* and control group (dashed line = 1). n = 5-12 (5-12 IVD biological replicates; 3 MSC biological replicates and 1-4 experimental replicates); [#] $p < 0.05$, [##] $p < 0.01$ (*versus* control); * $p < 0.05$, **** $p < 0.0001$ (between CTS + IL-1β stimulation and treatments).
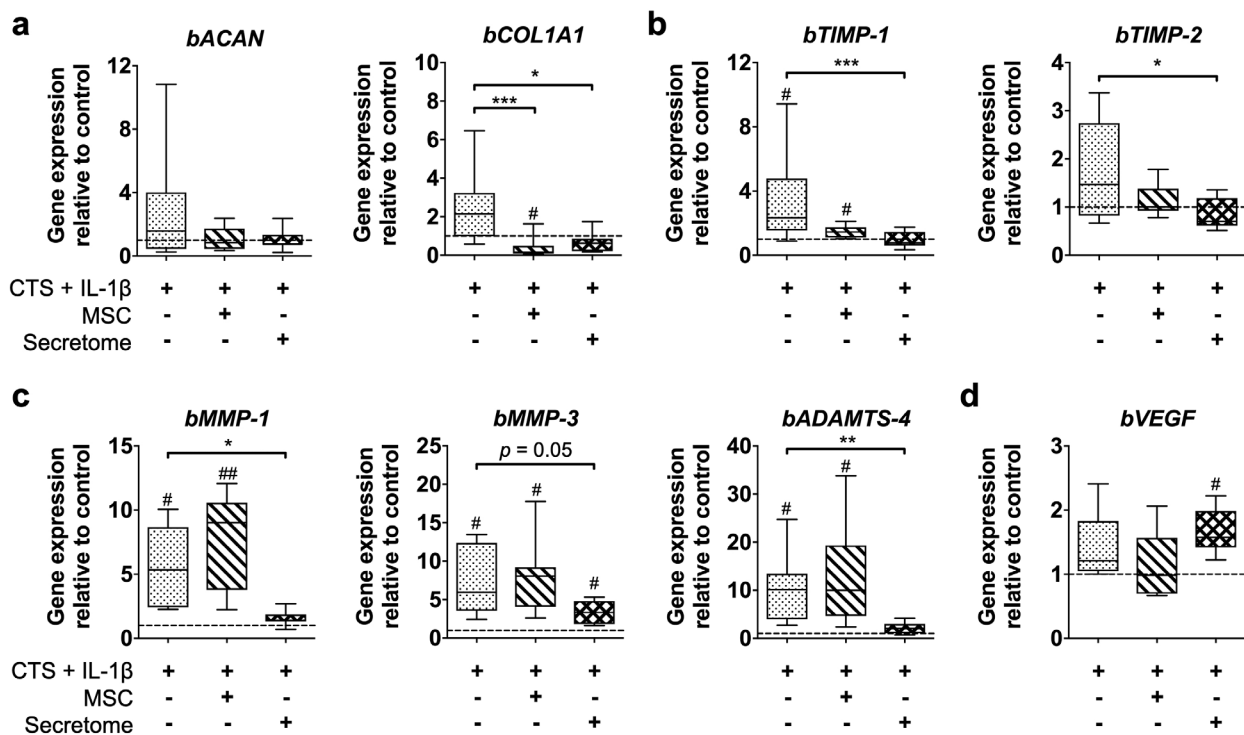

Fig. 3. Gene expression of bovine AF cells at day 11 of organ culture. (**a**) Relative mRNA expression of bovine matrix components, (**b**) TIMPs, (**c**) matrix degrading enzymes and (**d**) vascularisation marker *bVEGF*. Results were normalised to the expression level of *bGAPDH* and control group (dashed line = 1). n = 6-12 (6-12 IVD biological replicates; 3 MSC biological replicates and 2-4 experimental replicates); [#] $p < 0.05$, [##] $p < 0.01$, [###] $p < 0.001$ (*versus* control); * $p < 0.05$, ** $p < 0.01$, *** $p < 0.001$ (between CTS + IL-1β stimulation and treatments).

treated with MSCs (MSC group) or secretome of pre-conditioned MSCs (secretome group) to mimic the physiological conditions of MSCs in the AF-OC model.

To investigate whether AF cell viability was affected by CTS + IL-1β, co-culture with MSCs or secretome treatment after 4 d of organ culture, the expression of *bNOS2*, a marker of cell survival, was analysed (Fig. 2**a**). No differences were observed between the experimental groups. The proinflammatory markers *bIL-6*, *bIL-8* and *bPTGS2* were significantly upregulated in the CTS + IL-1β-treated group ($p < 0.05$) in comparison to the control group and to the combination with the secretome treatment ($p < 0.05$, Fig. 2**b**). The MSC group presented upregulated *bIL-6* and *bPTGS2* expression in comparison to the control group ($p < 0.05$) and upregulated *bIL-8* expression *versus* CTS + IL-1β stimulation alone ($p < 0.05$). Regarding the expression of inhibitory complement receptors (Fig. 2**c**), *bCD46*,

bCD55, and *bCD59* were upregulated after CTS + IL-1β stimulation when compared to control samples, this being statistically significant for *bCD59* ($p < 0.05$). The secretome treatment significantly downregulated *bCD46*, *bCD55* (both $p < 0.05$) and *bCD59* ($p < 0.0001$) expression in comparison to CTS + IL-1β stimulation alone. *bCD46* was upregulated in the MSC-treated group, whereas *bCD59* was downregulated in secretome-treated samples, both in comparison to the control group ($p < 0.01$).

The gene expression of the main AF matrix components *bACAN* and *bCOL1A1*, inhibitors of matrix degradation *bTIMP-1* and *bTIMP-2*, matrix degrading enzymes *bMMP-1*, *bMMP-3* and *bADAMTS-4* and the vascularisation marker *bVEGF* was also analysed (Fig. 3). While *bACAN* expression was not altered in the different groups, *bCOL1A1* was downregulated in the MSC group when compared to the control group ($p < 0.05$) and in the MSC ($p < 0.001$) and secretome ($p < 0.05$) groups *versus* the
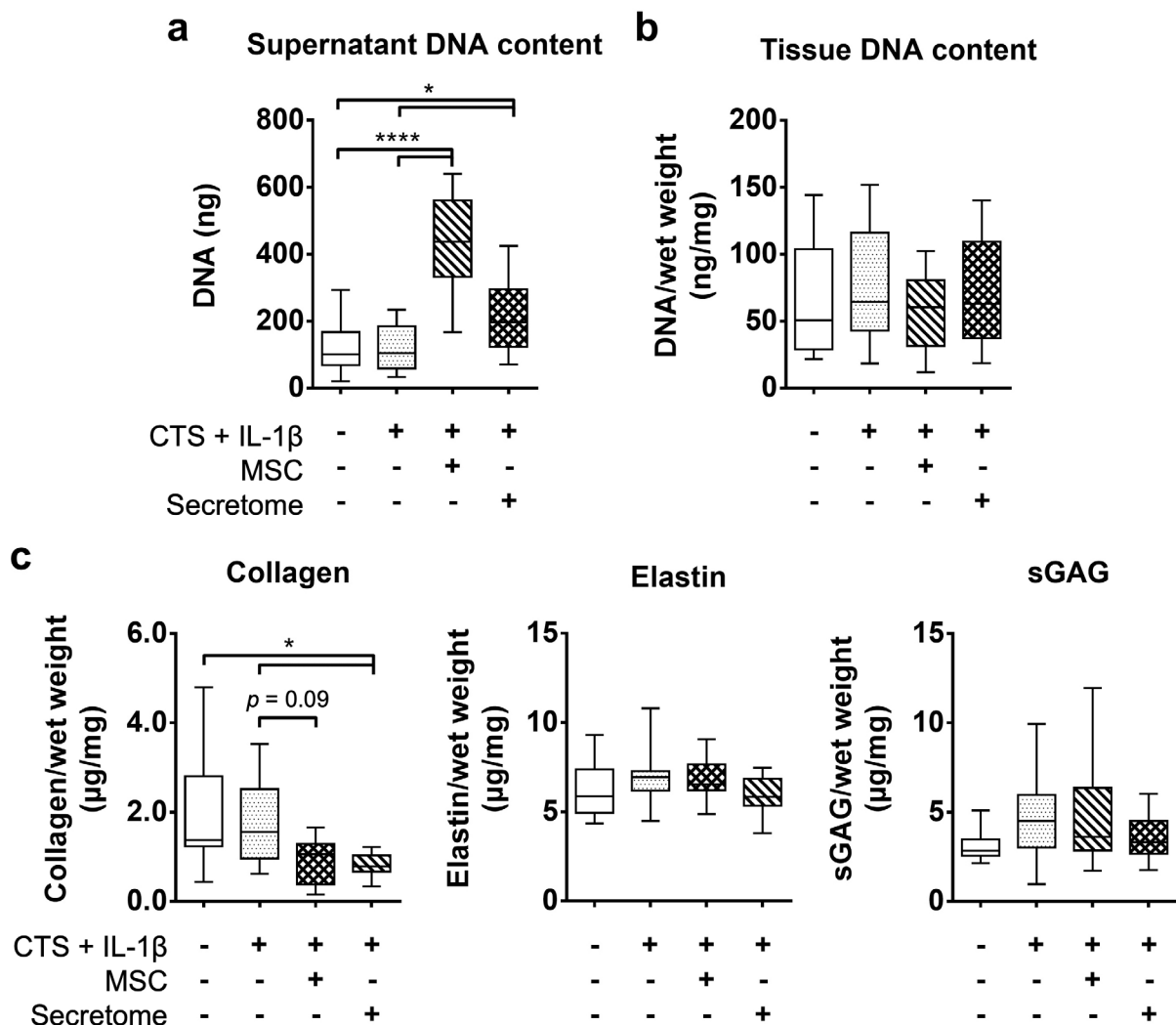

Fig. 4. DNA and protein content of AF-OCs at day 11. (**a**) Amount of DNA (ng) released to the culture supernatants. (**b**) DNA content in the AF tissues normalised to wet weight (ng/mg). (**c**) Collagen, elastin, and sGAG content in the AF tissues normalised to wet weight (µg/mg). n = 10-18 (6-12 IVD biological replicates and 1-2 experimental replicates; 3 MSC biological replicates and 3-6 experimental replicates), * $p < 0.05$, **** $p < 0.0001$.
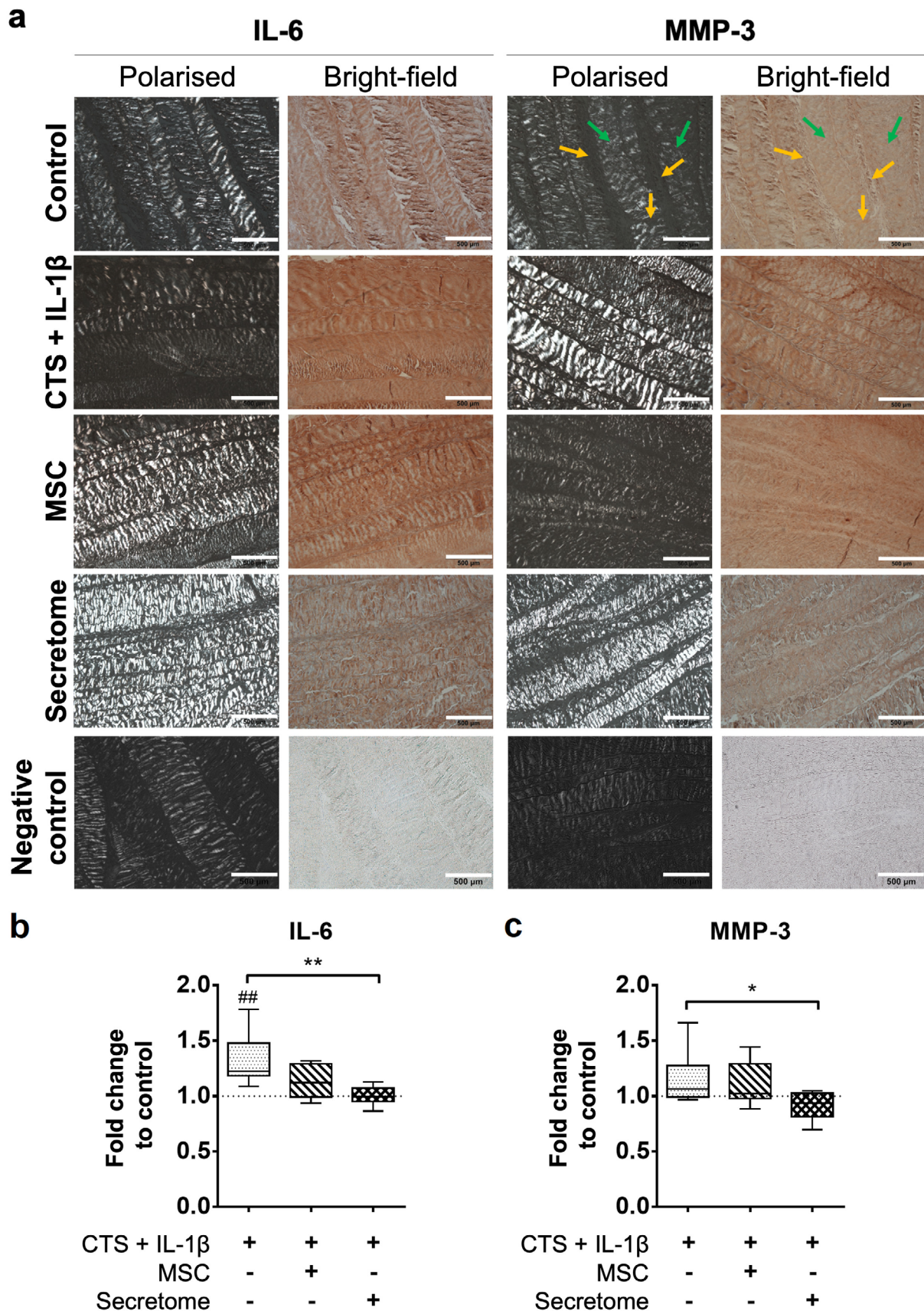
Fig. 5. IL-6 and MMP-3 content of AF-OCs at day 11. (**a**) Representative images under polarised-light and bright-field of the IL-6 and MMP-3 distribution within the TLBN (yellow arrows) and the LM (green arrows) of AF-OCs; scale bar: 500 μm. (**b**) IL-6 and (**c**) MMP-3 staining intensity in the TLBN normalised to the LM and to the unstimulated control sample for each experiment. *n* = 7-10 (7-10 IVD biological replicates; 3 MSC biological replicates and 2-4 experimental replicates); ## $p < 0.01$ (*versus* control, dashed line); * $p < 0.05$, ** $p < 0.01$ (between CTS + IL-1β stimulation and treatments).

CTS + IL-1β group (Fig. 3**a**). *bTIMP-1* was significantly upregulated by CTS + IL-1β stimulation and co-culture with MSCs (*p* < 0.05, Fig. 3**b**). *bTIMP-1* and *bTIMP*-2 were significantly downregulated by the secretome (*p* < 0.001) in comparison to CTS + IL-1β stimulation

alone. *bMMP-1*, *bMMP-3* and *bADAMTS-4* were upregulated in the CTS + IL-1β-stimulated and MSC-treated groups when compared to the control group (*p* < 0.05, Fig. 3**c**) but were downregulated by the combination with the secretome treatment
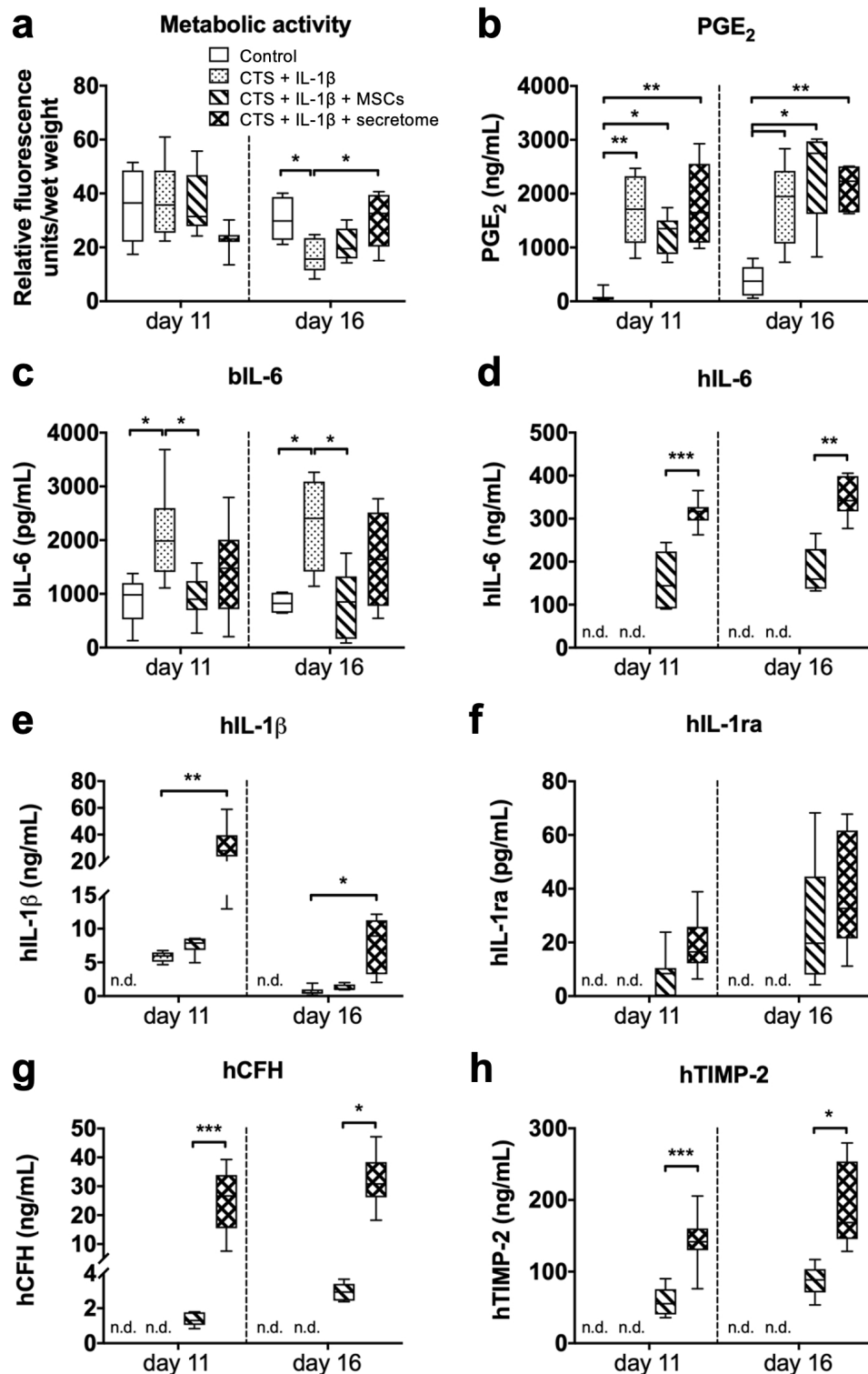

Fig. 6. Cell metabolic activity and protein content of AF-OC supernatants at days 11 and 16. At day 11, 50 % of the medium was exchanged. (**a**) Mitochondrial metabolic activity of AF-OCs expressed in relative fluorescence units normalised to tissue wet weight. (**b**) Human/bovine PGE_2 (ng/mL), (**c**) bIL-6 (pg/mL), (**d**) hIL-6 (ng/mL), (**e**) hIL-1β (ng/mL), (**f**) hIL-1ra (pg/mL), (**g**) hCFH (ng/mL) and (**h**) hTIMP-2 (ng/mL) concentrations. *n* = 6-12 (6-12 IVD biological replicates; 3 MSC biological replicates and 2-4 experimental replicates), * *p* < 0.05, ** *p* < 0.01, *** *p* < 0.001, n.d.: not detectable.

compared to CTS + IL-1β ($p \leq 0.05$). *bVEGF* expression was significantly upregulated with the secretome treatment in contrast to control samples ($p < 0.05$, Fig. 3**d**) but did not present differences compared to CTS + IL-1β.

AF matrix remodelling

Following 4 d of stimulation, no differences were found in the DNA content released to the culture supernatant between the CTS + IL-1β and control groups (Fig. 4**a**); whereas the groups treated with MSCs ($p < 0.0001$) or secretome ($p < 0.05$) displayed an increase in the DNA released to the culture supernatant. When the DNA content was quantified in the AF tissue itself, no differences were detected between the groups (Fig. 4**b**). Collagen, elastin and sGAG matrix content was also quantified in the AF tissue (Fig. 4**c**). Elastin and sGAG contents were similar under all conditions, whereas collagen content was slightly lower in the MSC-treated group ($p = 0.09$, *versus* CTS + IL-1β alone) and significantly lower in secretome-treated samples ($p < 0.05$, in comparison to both the control and CTS + IL-1β groups).

Production of soluble factors

The distribution of IL-6 and MMP-3 in the AF tissue was assessed by immunohistochemistry at day 11 (Fig. 5). IL-6 and MMP-3 were detected over the entire AF tissue (Fig. 5**a**). For IL-6, a significantly higher staining intensity was found in the CTS + IL-1β group in comparison to the control group ($p < 0.01$, Fig. 5**b**), which was reduced by secretome treatment ($p < 0.01$). A significantly higher staining intensity was also found for MMP3 on CTS + IL-1β stimulation alone in contrast to the secretome treatment ($p < 0.05$, Fig. 5**c**).

The mitochondrial metabolic activity of the cells, as well as PGE$_2$, bIL-6, hIL-6, IL-1β, IL-1ra, hCFH and hTIMP-2 content in the AF-OC supernatants were quantified at day 11 and 16 (Fig. 6). While at day 11 no significant differences were found in the mitochondrial metabolic activity of the cells (Fig. 6**a**), at day 16, significantly lower activity was observed in the CTS + IL-1β group ($p < 0.05$), which was recovered in the secretome treatment group ($p < 0.05$). PGE$_2$ production was higher in all stimulated/treated groups *versus* control samples after 4 (day 11) and 9 (day 16) d of culture ($p < 0.05$, Fig. 6**b**). Interestingly, bIL-6 production was higher after CTS + IL-1β stimulation than in control and co-culture with MSCs at both timepoints ($p < 0.05$, Fig. 6**c**). hIL-1β, hIL-6, hIL-1ra, hCFH and hTIMP-2 ELISAs detected specifically human molecules (Fig. 6**d**-**h**). Higher hIL-6, hCFH and hTIMP-2 were found in the supernatant of the secretome-treated group in comparison to the release by the MSCs in direct co-culture with the AF-OCs ($p < 0.05$). Slightly higher IL-1ra was detected in the secretome group but without significant differences. hIL-1β was added to the culture medium of all groups except for the control. At both timepoints of analysis, a slight consumption was observed in the CTS + IL-1β-stimulated and MSC-treated groups in comparison to the added 10 ng/mL, whereas significantly higher hIL-1β was observed in the secretome-treated group in comparison to CTS + IL-1β ($p < 0.05$). The detected hIL-1β was partially produced by the pre-conditioned MSCs, as well as IL-1ra (Fig. 7).
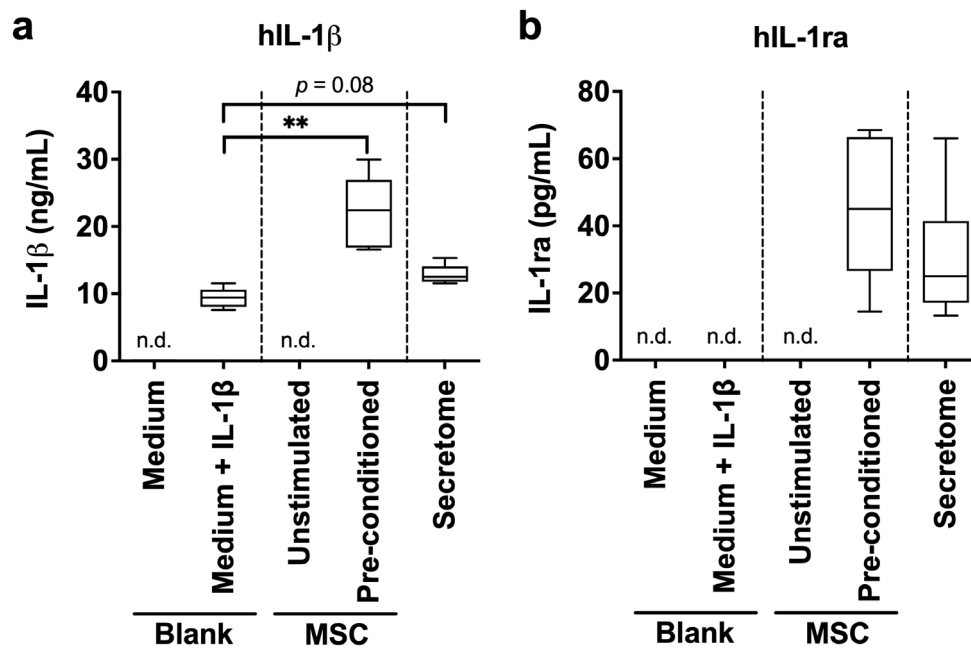

Fig. 7. Protein content of blank basal medium without or with 10 ng/mL IL-1β supplementation; of human MSC culture supernatants after 48 h of culture under basal medium and normoxia (unstimulated) or preconditioning (pre-conditioned); and of the secretome solution added to the AF organ cultures (secretome mixed in a 1 : 1 ratio with medium + IL-1β). (**a**) Human IL-1β (hIL-1β, ng/mL), and (**b**) hIL-1ra (pg/mL). $n = 6$ (3 biological replicates and 2 experimental replicates), n.d. = not detectable, ** $p < 0.01$, non-parametric Mann-Whitney test.

Mechanical properties of AF tissue

A biomechanical peel test was performed in AF tissue segments after 9 d of organ culture stimulation/treatment (Fig. 8). Force-displacement curves were obtained and the mean force along one or more plateau regions was used to calculate the mean annular delamination strength for each sample. No differences between the control and the CTS + IL-1β stimulation were observed at this timepoint. Approximately 30 % lower delamination strength was detected in the groups treated with MSCs ($p = 0.07$) and secretome ($p < 0.05$) when compared to the CTS + IL-1β stimulation alone.

Discussion

The healthy IVD is characterised by a harsh microenvironment, because of low oxygen levels, high osmolarity, nutritional deficits and mechanical loading. These conditions are further exacerbated by degeneration and inflammation (Molinos *et al.*, 2015; Urban, 2002). The proinflammatory/degenerative microenvironment, particularly low oxygen (5 % O_2) and low glucose (1 mmol/L) conditions have been shown to promote stem cell death and inhibit sGAG and collagen production *in vitro* (Naqvi and Buckley, 2015). In the present study, the proinflammatory and catabolic environment of the IVD was simulated following a previously established *ex vivo* model of bovine AF rings cultured under low oxygen and glucose supplies, iso-osmotic (400 mOsm) conditions and CTS + IL-1β stimulation (Saggese *et al.*, 2019). However, in the present study, in contrast to Saggese *et al.* (2019), the AF rings were stimulated with 10 ng/

mL instead of 1 ng/mL IL-1β and a longer stimulation period of up to 9 d was investigated. The stimulation with 10 ng/mL IL-1β was previously established for MSCs (Ferreira *et al.*, 2021) and is still in the range of concentrations used by other authors (Le Maitre *et al.*, 2007; Markova *et al.*, 2013; Ponnappan *et al.*, 2011). While IL-1β seemed to be consumed/degraded with time in culture (Fig. 6**e** in contrast to the initial concentration of the medium + IL-1β in Fig. 7**a**), the overall expression/production of proinflammatory molecules and matrix-degrading enzymes by AF cells increased after CTS + IL-1β stimulation (as shown in Fig. 2**b**, 3**c**, 5, 6**b**,**c**). Similarly, the model established by Saggese *et al.* (2019) was also characterised by an increased production of COX-2, PGE_2, IL-6 and MMP-3. Interestingly, a decrease in mitochondrial metabolic activity was observed in the CTS + IL-1β group after 16 d of culture (Fig. 6**a**), which has been previously related with inflammation (Hernández-Aguilera *et al.*, 2013) and AF cell apoptosis (Rannou *et al.*, 2004). But by contrast, cell viability was unaffected, because a similar DNA content was observed for the different groups (Fig. 4**b**), in agreement with findings from Saggese *et al.* (2019).

Regarding the expression of complement regulatory proteins that play an important role in the innate immune response, only *bCD59* was upregulated after CTS + IL-1β stimulation (Fig. 2**c**), with no changes observed for *bCD46* or *bCD55* (important for cell protection against complement-mediated lysis). Interestingly, CTS appeared to have a stronger impact on the regulation of these factors than IL-1β (data not shown). By contrast, IL-1β stimulation alone has been previously described to upregulate the expression of these regulators by isolated human articular chondrocytes (Hyc *et al.*, 2003); however, chondrocyte gene expression was investigated only 24 h after stimulation. Nevertheless, the present study results suggested that, because CD59 is a direct TCC inhibitor, the pathway leading to its formation may play a role in IVD degeneration. This is in agreement with recent findings in human degenerated IVD tissues (Teixeira *et al.*, 2021).

In CTS + IL-1β-stimulated AF-OCs, no changes in *bACAN* or *bCOL1A1* gene expression (Fig. 3**a**) or collagen, elastin or sGAG matrix content (Fig. 4**c**) were detected in comparison to non-stimulated AF-OCs. Moreover, a slight increase in the annular delamination strength was observed in CTS + IL-1β-stimulated AF-OCs (3.1 ± 1.0 N/mm, Fig. 7) in comparison to the unstimulated control (2.6 ± 1.2 N/mm) after 9 d of stimulation (but without statistical significance). Interestingly, in the study by Saggese *et al.* (2019), no changes in the tissue's fibrillin-1 content were detected after 5 d of CTS + IL-1β stimulation in comparison to untreated controls. However, a decrease in the annular peel strength from ~ 1.25 N/mm in the control group to ~ 0.8 N/mm in the CTS + IL-1β group was detected (Saggese *et al.*, 2019). It appears that, with time in culture, tissues displayed higher delamination strength values in comparison
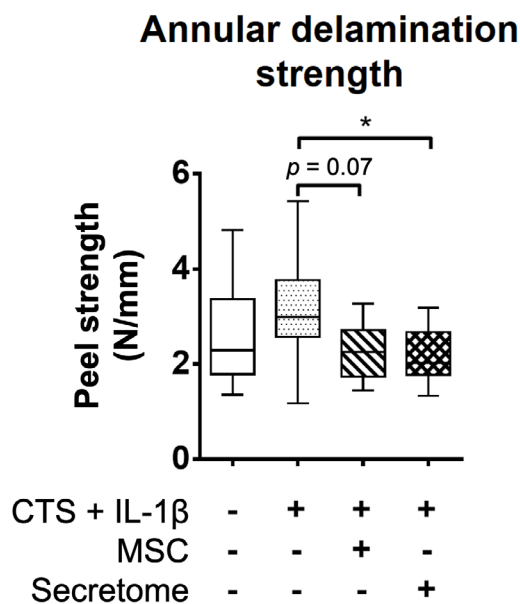

Annular delamination strength

Fig. 8. Annular delamination strength of AF-OCs at day 16. Peel strength as a function of the displacement rate (N/mm). *n* = 6-12 (6-12 IVD biological replicates; 3 MSC biological replicates and 2-4 experimental replicates), * *p* < 0.05.

to the data previously published by Saggese *et al.* (2019). This might indicate that changes in other factors which were not the subject of the present study (*e.g.* versican, collagen type VI) (Melrose *et al.*, 2008) may have contributed to the differences in the peel-force test at the different timepoints. Therefore, to more closely simulate the human physiological conditions and induce matrix breakdown and annular tear, a model using higher strains and complex loading (Heuer *et al.*, 2008) could be used in future investigations.

MSC-based therapies have been investigated for IVD regeneration and back pain treatment because of i) the MSC ability to differentiate in response to the microenvironment and cell-cell interaction into an NP-like phenotype, promoting matrix synthesis (Strassburg *et al.*, 2010), and ii) their anti-inflammatory and immune-modulatory activities (Cunha *et al.*, 2017; Miguélez-Rivera *et al.*, 2018; Teixeira *et al.*, 2018). Clinical trials have shown an increased IVD water content and an improvement of pain and disability in up to 2 years of follow-up (Noriega *et al.*, 2017; Orozco *et al.*, 2011; Pettine *et al.*, 2015; Pettine *et al.*, 2016; Yoshikawa *et al.*, 2010). These therapies have mostly focused on restoring extracellular matrix production (particularly ACAN) and disc biomechanics (Adams and Roughley, 2006; Bendtsen *et al.*, 2016), but still little is known regarding the biological effects of MSC transplantation. Moreover, few studies have addressed/targeted a functional AF repair (Sakai and Grad, 2015). MSCs secrete numerous soluble factors in response to the microenvironmental cues, tuning several mechanisms in neighbour tissues *via* paracrine signalling (Ferreira *et al.*, 2018). Therefore, the therapeutic potential of MSC secretome has been investigated in the context of several disorders, including degenerative joint diseases (Ferreira *et al.*, 2018). MSC secretome has been suggested to stimulate IVD progenitor cells activity towards repair in degenerated human IVD tissues (Brisby *et al.*, 2013). Nonetheless, the MSC secretome content may be determined by the microenvironment to which the cells are exposed (Ferreira *et al.*, 2018). Therefore, the effect of MSCs *versus* pre-conditioned MSC secretome was evaluated in the present study.

MSCs were exposed to a low oxygen atmosphere (6 % O_2) and proinflammatory stimulus (IL-1β medium supplementation), features of the AF-OC microenvironment. The pre-conditioned MSCs displayed upregulated expression of the proinflammatory markers *hIL-6* and *hIL-8* and the matrix degrading enzymes *hMMP-1* and *hMMP-3* (data not shown). In particular, IL-1β-preconditioning has been shown to significantly upregulate the expression of multiple immune-modulating cytokines (*e.g.* COX-2, IL-6, IL-8) and chemokines (*e.g.* CCL5), as well as MMPs compared to non-stimulated MSCs (Carrero *et al.*, 2012; Fan *et al.*, 2012; Ferreira *et al.*, 2021). Interestingly, the complement components *hC3* and *hC5* and regulatory proteins were also shown to be upregulated by the pre-conditioned

MSCs, whereas TCC components *hC6* and *hC9* were downregulated in comparison to MSCs cultured under atmospheric oxygen conditions and normal expansion medium (data not shown). This indicates a potential to modulate the complement system activation to a certain extent, in agreement with previous findings (Ignatius *et al.*, 2011; Soland *et al.*, 2013). Data from the supernatants of secretome-treated AF-OCs (evaluated by ELISA assays without cross-reactivity with bovine molecules) confirmed that preconditioned MSCs produced high concentrations of immune-modulating molecules (Fig. 6), including hIL-6 and hCFH – a first line of complement inhibition (Tu *et al.*, 2010) – as well as hTIMP-2 – a tissue damage mediator. IL-1β and IL-1ra were also produced by pre-conditioned MSCs (Fig. 7). Although IL-1ra has been shown to inhibit IL-1β proinflammatory and catabolic effects when 200 μg/mL were delivered directly onto explants of human degenerate IVDs (Le Maitre *et al.*, 2005, 2007), the concentration produced by pre-conditioned MSCs was very low (in the pg/mL range). Therefore, IL-1ra was not expected to have a strong inhibitory effect.

A paracrine immunomodulatory effect of MSC secretome has been described in osteoarthritic cartilage explant cultures (van Buul *et al.*, 2012) and in rat NP/AF cell and macrophage co-cultures (Miguélez-Rivera *et al.*, 2018), and it was confirmed in the present study in the AF-OCs. Molecules produced by the pre-conditioned MSCs contributed to a down-regulation of *bIL-6*, *bIL-8* and *bPTGS2*, as well as of *bCD46*, *bCD55* and *bCD59* by AF cells (Fig. 2**b**,**c**). Interestingly, human/bovine PGE_2 production (Fig. 6**b**) increased with the CTS + IL-1β but was not altered by MSC or secretome treatments even though *bPTGS2* was downregulated (Fig. 2**b**). PGE_2 is highly produced by both MSCs and IVD cells after IL-1β stimulation (Teixeira *et al.*, 2018), in agreement with the present study. By contrast, few effects were observed with MSCs in co-culture when compared to previous findings in which IVD cells displayed a less proinflammatory phenotype in a static model of MSCs and IVD tissue co-cultures (Teixeira *et al.*, 2018). Although the MSC-seeded AF-OC rings were maintained under static conditions for 24 h after seeding to promote cell adhesion, significantly higher DNA content was found in the supernatant of this group (Fig. 4**a**), indicating cell detachment. Moreover, the adaptation of the surviving MSCs to the new environment, particularly the dynamic loading, may have affected their anti-inflammatory phenotype and regenerative potential.

In the presence of the MSC secretome, a down-regulation of matrix-degrading enzymes and their inhibitors by AF cells (Fig. 3**b**,**c**), and a decrease in the bovine/human MMP-3 content in the CTS + IL-1β-stimulated AF tissue was observed (Fig. 5**b**). Nevertheless, the secretome also contributed to a weakening of the AF peeling strength, which tended to increase under CTS + IL-1β treatment (Fig. 8). Although no differences were found between the

MSC-treated group and the control group regarding peeling strength, less collagen was detected at the gene and/or protein level (Fig. 3**a**,4**c**, respectively). Because collagen is an important structural protein with an impact on the AF mechanical properties, alterations after secretome treatment will be further investigated in this model and *in vivo* to better understand its physiological relevance. The study results were in contrast with *in vivo* studies showing that the MSC secretome may reduce cartilage damage in arthritic mice by reducing ACAN cleavage (Kay *et al.*, 2017) and MMP-13 expression (Chen *et al.*, 2019). Moreover, MSCs-derived exosomes have also been shown to increase ACAN and COL2 and decrease MMP-13 expression by chondrocytes isolated from a murine osteoarthritis model (Liu *et al.*, 2018) and to upregulate ACAN and COL2 by human NP cells (Lu *et al.*, 2017).

Another important aspect to be addressed is angiogenesis/vascularisation, which, while beneficial for tissue repair/regeneration in vascularised tissues, is known to contribute to IVD-degeneration-associated back pain (Binch *et al.*, 2014). Although vascularisation could not be investigated in the stretched AF-OC model, *bVEGF* was upregulated in AF cells treated with secretome *versus* control (Fig. 3**d**). Nevertheless, the secretome did not appear to affect sprouting of human endothelial cells (data not shown). Data did not provide enough evidence on the role of the preconditioned secretome in angiogenesis; however, IL-1β and MSC secretome have been shown to upregulate the expression of pro-angiogenic factors by endothelial cells (Fan *et al.*, 2004; Rosell *et al.*, 2009), but without a functional effect (Fan *et al.*, 2004).

The limitations of the present study include the proinflammatory degenerative microenvironment of the disc, which cannot be completely simulated, and the short investigation time in which the simulation of a therapy in a long-term perspective is not possible. Additionally, the communication between MSCs and cells of the immune system cannot be simulated using this model. Moreover, the tensile strain applied to the system might have contributed to reduced MSC adhesion to the AF rings with time in culture and, therefore, explain why almost no effects were found in the co-culture group.

Overall, the MSC secretome had a potent anti-inflammatory effect on the phenotype of AF cells stimulated with CTS + IL-1β, which was, therefore, mediated by a paracrine mechanism. It also had an effect on collagen production/degradation, particularly *COL1A1*, as well as on the AF mechanical properties compared to CTS + IL-1β. Future work will investigate the long-term effect of the secretome on the AF matrix.

Conclusions

AF cells presented a proinflammatory and catabolic phenotype after CTS + IL-1β stimulation for 4 d but without changes in sGAG, elastin or collagen tissue content. Treatment with the MSC secretome (following preconditioning by 10 ng/mL IL-1β medium supplementation and culture under 6 % O_2 and 8.5 % CO_2 for 48 h) contributed to a decrease in the inflammatory and catabolic status of AF cells activated by CTS + IL-1β and it also appeared to modulate the activation of cellular complement system regulators. However, the MSC secretome contributed to a decrease in collagen at the gene/protein level and a reduction in the AF delamination strength in comparison to the CTS + IL-1β stimulation. Ongoing studies with extended culture periods are necessary to evaluate long-term changes in the AF matrix at the protein level and alterations of mechanical properties.

References

Adams MA, Roughley PJ (2006) What is intervertebral disc degeneration, and what causes it? Spine (Phila Pa 1976) **31**: 2151-2161.

Bendtsen M, Bunger C, Colombier P, Le Visage C, Roberts S, Sakai D, Urban JP (2016) Biological challenges for regeneration of the degenerated disc using cellular therapies. Acta Orthop **87**: 39-46.

Binch AL, Cole AA, Breakwell LM, Michael AL, Chiverton N, Cross AK, Le Maitre CL (2014) Expression and regulation of neurotrophic and angiogenic factors during human intervertebral disc degeneration. Arthritis Res Ther **16**: 416. DOI: 10.1186/s13075-014-0416-1.

Brisby H, Papadimitriou N, Brantsing C, Bergh P, Lindahl A, Barreto Henriksson H (2013) The presence of local mesenchymal progenitor cells in human degenerated intervertebral discs and possibilities to influence these *in vitro*: a descriptive study in humans. Stem Cells Dev **22**: 804-814.

Carrero R, Cerrada I, Lledó E, Dopazo J, García-García F, Rubio MP, Trigueros C, Dorronsoro A, Ruiz-Sauri A, Montero JA, Sepúlveda P (2012) IL1β induces mesenchymal stem cells migration and leucocyte chemotaxis through NF-κB. Stem Cell Rev Rep **8**: 905-916.

Chen W, Sun Y, Gu X, Hao Y, Liu X, Lin J, Chen J, Chen S (2019) Conditioned medium of mesenchymal

stem cells delays osteoarthritis progression in a rat model by protecting subchondral bone, maintaining matrix homeostasis, and enhancing autophagy. J Tissue Eng Regen Med **13**: 1618-1628.

Cunha C, Almeida CR, Almeida MI, Silva AM, Molinos M, Lamas S, Pereira CL, Teixeira GQ, Monteiro AT, Santos SG, Gonçalves RM, Barbosa MA (2017) Systemic delivery of bone marrow mesenchymal stem cells for *in situ* intervertebral disc regeneration. Stem Cells Transl Med **6**: 1029-1039.

Dai W, Hale SL, Kloner RA (2007) Role of a paracrine action of mesenchymal stem cells in the improvement of left ventricular function after coronary artery occlusion in rats. Regen Med **2**: 63-68.

Fan F, Stoeltzing O, Liu W, McCarty MF, Jung YD, Reinmuth N, Ellis LM (2004) Interleukin-1beta regulates angiopoietin-1 expression in human endothelial cells. Cancer Res **64**: 3186-3190.

Fan H, Zhao G, Liu L, Liu F, Gong W, Liu X, Yang L, Wang J, Hou Y (2012) Pre-treatment with IL-1β enhances the efficacy of MSC transplantation in DSS-induced colitis. Cell Mol Immunol **9**: 473-481.

Ferreira JR, Teixeira GQ, Neto E, Ribeiro-Machado C, Silva AM, Caldeira J, Leite Pereira C, Bidarra S, Maia AF, Lamghari M, Barbosa MA, Gonçalves RM (2021) IL-1β-pre-conditioned mesenchymal stem/stromal cells' secretome modulates the inflammatory response and aggrecan deposition in intervertebral disc. Eur Cell Mater **41**: 431-453.

Ferreira JR, Teixeira GQ, Santos SG, Barbosa MA, Almeida-Porada G, Goncalves RM (2018) Mesenchymal stromal cell secretome: influencing therapeutic potential by cellular pre-conditioning. Front Immunol **9**: 2837. DOI: 10.3389/fimmu.2018.02837.

Gregory DE, Bae WC, Sah RL, Masuda K (2012) Anular delamination strength of human lumbar intervertebral disc. Eur Spine J **21**: 1716-1723.

Grönblad M, Habtemariam A, Virri J, Seitsalo S, Vanharanta H, Guyer RD (2003) Complement membrane attack complexes in pathologic disc tissues. Spine (Phila Pa 1976) **28**: 114-118.

Hernández-Aguilera A, Rull A, Rodríguez-Gallego E, Riera-Borrull M, Luciano-Mateo F, Camps J, Menéndez JA, Joven J (2013) Mitochondrial dysfunction: a basic mechanism in inflammation-related non-communicable diseases and therapeutic opportunities. Mediators Inflamm **2013**: 135698. DOI: 10.1155/2013/135698.

Heuer F, Schmidt H, Wilke H-J (2008) The relation between intervertebral disc bulging and annular fiber associated strains for simple and complex loading. J Biomech **41**: 1086-1094.

Hyc A, Osiecka-Iwan A, Strzelczyk P, Moskalewski S (2003) Effect of IL-1beta, TNF-alpha and IL-4 on complement regulatory protein mRNA expression in human articular chondrocytes. Int J Mol Med **11**: 91-94.

Ignatius A, Schoengraf P, Kreja L, Liedert A, Recknagel S, Kandert S, Brenner RE, Schneider M, Lambris JD, Huber-Lang M (2011) Complement

C3a and C5a modulate osteoclast formation and inflammatory response of osteoblasts in synergism with IL-1β. J Cell Biochem **112**: 2594-2605.

Kay AG, Long G, Tyler G, Stefan A, Broadfoot SJ, Piccinini AM, Middleton J, Kehoe O (2017) Mesenchymal stem cell-conditioned medium reduces disease severity and immune responses in inflammatory arthritis. Sci Rep **7**: 18019. DOI: 10.1038/s41598-017-18144-w.

Krampera M, Cosmi L, Angeli R, Pasini A, Liotta F, Andreini A, Santarlasci V, Mazzinghi B, Pizzolo G, Vinante F, Romagnani P, Maggi E, Romagnani S, Annunziato F (2006) Role for interferon-gamma in the immunomodulatory activity of human bone marrow mesenchymal stem cells. Stem Cells **24**: 386-398.

Le Maitre CL, Freemont AJ, Hoyland JA (2005) The role of interleukin-1 in the pathogenesis of human intervertebral disc degeneration. Arthritis Res Ther **7**: R732-745.

Le Maitre CL, Hoyland JA, Freemont AJ (2007) Interleukin-1 receptor antagonist delivered directly and by gene therapy inhibits matrix degradation in the intact degenerate human intervertebral disc: an *in situ* zymographic and gene therapy study. Arthritis Res Ther **9**: R83. DOI: 10.1186/ar2282.

Li W, Ren G, Huang Y, Su J, Han Y, Li J, Chen X, Cao K, Chen Q, Shou P, Zhang L, Yuan Z-R, Roberts AI, Shi S, Le AD, Shi Y (2012) Mesenchymal stem cells: a double-edged sword in regulating immune responses. Cell Death Differ **19**: 1505-1513.

Liu Y, Lin L, Zou R, Wen C, Wang Z, Lin F (2018) MSC-derived exosomes promote proliferation and inhibit apoptosis of chondrocytes *via* lncRNA-KLF3-AS1/miR-206/GIT1 axis in osteoarthritis. Cell Cycle **17**: 2411-2422.

Livak KJ, Schmittgen TD (2001) Analysis of relative gene expression data using real-time quantitative PCR and the 2(-Delta Delta C(T)) Method. Methods **25**: 402-408.

Lu K, Li HY, Yang K, Wu JL, Cai XW, Zhou Y, Li CQ (2017) Exosomes as potential alternatives to stem cell therapy for intervertebral disc degeneration: *in-vitro* study on exosomes in interaction of nucleus pulposus cells and bone marrow mesenchymal stem cells. Stem Cell Res Ther **8**: 108. DOI: 10.1186/s13287-017-0563-9.

Markova DZ, Kepler CK, Addya S, Murray HB, Vaccaro AR, Shapiro IM, Anderson DG, Albert TJ, Risbud MV (2013) An organ culture system to model early degenerative changes of the intervertebral disc II: profiling global gene expression changes. Arthritis Res Ther **15**: R121. DOI: 10.1186/ar4301.

Melrose J, Smith SM, Appleyard RC, Little CB (2008) Aggrecan, versican and type VI collagen are components of annular translamellar crossbridges in the intervertebral disc. Eur Spine J **17**: 314-324.

Miguélez-Rivera L, Pérez-Castrillo S, González-Fernández ML, Prieto-Fernández JG, López-González ME, García-Cosamalón J, Villar-Suárez V (2018) Immunomodulation of mesenchymal stem cells in discogenic pain. Spine J **18**: 330-342.

Molinos M, Almeida CR, Caldeira J, Cunha C, Gonçalves RM, Barbosa MA (2015) Inflammation in intervertebral disc degeneration and regeneration. J R Soc Interface **12**: 20141191. DOI: 10.1098/rsif.2014.1191.

Moradi-Lakeh M, Forouzanfar MH, Vollset SE, El Bcheraoui C, Daoud F, Afshin A, Charara R, Khalil I, Higashi H, Abd El Razek MM, Kiadaliri AA, Alam K, Akseer N, Al-Hamad N, Ali R, AlMazroa MA, Alomari MA, Al-Rabeeah AA, Alsharif U, Altirkawi KA, Atique S, Badawi A, Barrero LH, Basulaiman M, Bazargan-Hejazi S, Bedi N, Bensenor IM, Buchbinder R, Danawi H, Dharmaratne SD, Zannad F, Farvid MS, Fereshtehnejad SM, Farzadfar F, Fischer F, Gupta R, Hamadeh RR, Hamidi S, Horino M, Hoy DG, Hsairi M, Husseini A, Javanbakht M, Jonas JB, Kasaeian A, Khan EA, Khubchandani J, Knudsen AK, Kopec JA, Lunevicius R, Abd El Razek HM, Majeed A, Malekzadeh R, Mate K, Mehari A, Meltzer M, Memish ZA, Mirarefin M, Mohammed S, Naheed A, Obermeyer CM, Oh IH, Park EK, Peprah EK, Pourmalek F, Qorbani M, Rafay A, Rahimi-Movaghar V, Shiri R, Rahman SU, Rai RK, Rana SM, Sepanlou SG, Shaikh MA, Shiue I, Sibai AM, Silva DAS, Singh JA, Skogen JC, Terkawi AS, Ukwaja KN, Westerman R, Yonemoto N, Yoon SJ, Younis MZ, Zaidi Z, Zaki MES, Lim SS, Wang H, Vos T, Naghavi M, Lopez AD, Murray CJL, Mokdad AH (2017) Burden of musculoskeletal disorders in the eastern Mediterranean region, 1990-2013: findings from the global burden of disease study 2013. Ann Rheum Dis **76**: 1365-1373.

Murray CJ, Barber RM, Foreman KJ, Abbasoglu Ozgoren A, Abd-Allah F, Abera SF, Aboyans V, Abraham JP, Abubakar I, Abu-Raddad LJ, Abu-Rmeileh NM, Achoki T, Ackerman IN, Ademi Z, Adou AK, Adsuar JC, Afshin A, Agardh EE, Alam SS, Alasfoor D, Albittar MI, Alegretti MA, Alemu ZA, Alfonso-Cristancho R, Alhabib S, Ali R, Alla F, Allebeck P, Almazroa MA, Alsharif U, Alvarez E, Alvis-Guzman N, Amare AT, Ameh EA, Amini H, Ammar W, Anderson HR, Anderson BO, Antonio CA, Anwari P, Arnlöv J, Arsic Arsenijevic VS, Artaman A, Asghar RJ, Assadi R, Atkins LS, Avila MA, Awuah B, Bachman VF, Badawi A, Bahit MC, Balakrishnan K, Banerjee A, Barker-Collo SL, Barquera S, Barregard L, Barrero LH, Basu A, Basu S, Basulaiman MO, Beardsley J, Bedi N, Beghi E, Bekele T, Bell ML, Benjet C, Bennett DA, Bensenor IM, Benzian H, Bernabé E, Bertozzi-Villa A, Beyene TJ, Bhala N, Bhalla A, Bhutta ZA, Bienhoff K, Bikbov B, Biryukov S, Blore JD, Blosser CD, Blyth FM, Bohensky MA, Bolliger IW, Bora Başara B, Bornstein NM, Bose D, Boufous S, Bourne RR, Boyers LN, Brainin M, Brayne CE, Brazinova A, Breitborde NJ, Brenner H, Briggs AD, Brooks PM, Brown JC, Brugha TS, Buchbinder R, Buckle GC, Budke CM, Bulchis A, Bulloch AG, Campos-Nonato IR, Carabin H, Carapetis JR, Cárdenas R, Carpenter DO, Caso V, Castañeda-Orjuela CA, Castro RE, Catalá-López F, Cavalleri F, Çavlin A, Chadha VK, Chang JC, Charlson FJ, Chen H, Chen W, Chiang PP, Chimed-Ochir O, Chowdhury R, Christensen H, Christophi CA, Cirillo M, Coates MM, Coffeng LE, Coggeshall MS, Colistro V, Colquhoun SM, Cooke GS, Cooper C, Cooper LT, Coppola LM, Cortinovis M, Criqui MH, Crump JA, Cuevas-Nasu L, Danawi H, Dandona L, Dandona R, Dansereau E, Dargan PI, Davey G, Davis A, Davitoiu DV, Dayama A, De Leo D, Degenhardt L, Del Pozo-Cruz B, Dellavalle RP, Deribe K, Derrett S, Des Jarlais DC, Dessalegn M, Dharmaratne SD, Dherani MK, Diaz-Torné C, Dicker D, Ding EL, Dokova K, Dorsey ER, Driscoll TR, Duan L, Duber HC, Ebel BE, Edmond KM, Elshrek YM, Endres M, Ermakov SP, Erskine HE, Eshrati B, Esteghamati A, Estep K, Faraon EJ, Farzadfar F, Fay DF, Feigin VL, Felson DT, Fereshtehnejad SM, Fernandes JG, Ferrari AJ, Fitzmaurice C, Flaxman AD, Fleming TD, Foigt N, Forouzanfar MH, Fowkes FG, Paleo UF, Franklin RC, Fürst T, Gabbe B, Gaffikin L, Gankpé FG, Geleijnse JM, Gessner BD, Gething P, Gibney KB, Giroud M, Giussani G, Gomez Dantes H, Gona P, González-Medina D, Gosselin RA, Gotay CC, Goto A, Gouda HN, Graetz N, Gugnani HC, Gupta R, Gupta R, Gutiérrez RA, Haagsma J, Hafezi-Nejad N, Hagan H, Halasa YA, Hamadeh RR, Hamavid H, Hammami M, Hancock J, Hankey GJ, Hansen GM, Hao Y, Harb HL, Haro JM, Havmoeller R, Hay SI, Hay RJ, Heredia-Pi IB, Heuton KR, Heydarpour P, Higashi H, Hijar M, Hoek HW, Hoffman HJ, Hosgood HD, Hossain M, Hotez PJ, Hoy DG, Hsairi M, Hu G, Huang C, Huang JJ, Husseini A, Huynh C, Iannarone ML, Iburg KM, Innos K, Inoue M, Islami F, Jacobsen KH, Jarvis DL, Jassal SK, Jee SH, Jeemon P, Jensen PN, Jha V, Jiang G, Jiang Y, Jonas JB, Juel K, Kan H, Karch A, Karema CK, Karimkhani C, Karthikeyan G, Kassebaum NJ, Kaul A, Kawakami N, Kazanjan K, Kemp AH, Kengne AP, Keren A, Khader YS, Khalifa SE, Khan EA, Khan G, Khang YH, Kieling C, Kim D, Kim S, Kim Y, Kinfu Y, Kinge JM, Kivipelto M, Knibbs LD, Knudsen AK, Kokubo Y, Kosen S, Krishnaswami S, Kuate Defo B, Kucuk Bicer B, Kuipers EJ, Kulkarni C, Kulkarni VS, Kumar GA, Kyu HH, Lai T, Lalloo R, Lallukka T, Lam H, Lan Q, Lansingh VC, Larsson A, Lawrynowicz AE, Leasher JL, Leigh J, Leung R, Levitz CE, Li B, Li Y, Li Y, Lim SS, Lind M, Lipshultz SE, Liu S, Liu Y, Lloyd BK, Lofgren KT, Logroscino G, Looker KJ, Lortet-Tieulent J, Lotufo PA, Lozano R, Lucas RM, Lunevicius R, Lyons RA, Ma S, Macintyre MF, Mackay MT, Majdan M, Malekzadeh R, Marcenes W, Margolis DJ, Margono C, Marzan MB, Masci JR, Mashal MT, Matzopoulos R, Mayosi BM, Mazorodze TT, McGill NW, McGrath JJ, McKee M, McLain A, Meaney PA, Medina C, Mehndiratta MM, Mekonnen W, Melaku YA, Meltzer M, Memish ZA, Mensah GA, Meretoja A, Mhimbira FA, Micha R, Miller TR, Mills EJ, Mitchell PB, Mock CN, Mohamed Ibrahim N, Mohammad KA, Mokdad AH, Mola GL, Monasta L, Montañez Hernandez JC, Montico M, Montine TJ, Mooney MD, Moore AR, Moradi-Lakeh M, Moran AE, Mori R, Moschandreas J, Moturi WN, Moyer

ML, Mozaffarian D, Msemburi WT, Mueller UO, Mukaigawara M, Mullany EC, Murdoch ME, Murray J, Murthy KS, Naghavi M, Naheed A, Naidoo KS, Naldi L, Nand D, Nangia V, Narayan KM, Nejjari C, Neupane SP, Newton CR, Ng M, Ngalesoni FN, Nguyen G, Nisar MI, Nolte S, Norheim OF, Norman RE, Norrving B, Nyakarahuka L, Oh IH, Ohkubo T, Ohno SL, Olusanya BO, Opio JN, Ortblad K, Ortiz A, Pain AW, Pandian JD, Panelo CI, Papachristou C, Park EK, Park JH, Patten SB, Patton GC, Paul VK, Pavlin BI, Pearce N, Pereira DM, Perez-Padilla R, Perez-Ruiz F, Perico N, Pervaiz A, Pesudovs K, Peterson CB, Petzold M, Phillips MR, Phillips BK, Phillips DE, Piel FB, Plass D, Poenaru D, Polinder S, Pope D, Popova S, Poulton RG, Pourmalek F, Prabhakaran D, Prasad NM, Pullan RL, Qato DM, Quistberg DA, Rafay A, Rahimi K, Rahman SU, Raju M, Rana SM, Razavi H, Reddy KS, Refaat A, Remuzzi G, Resnikoff S, Ribeiro AL, Richardson L, Richardus JH, Roberts DA, Rojas-Rueda D, Ronfani L, Roth GA, Rothenbacher D, Rothstein DH, Rowley JT, Roy N, Ruhago GM, Saeedi MY, Saha S, Sahraian MA, Sampson UK, Sanabria JR, Sandar L, Santos IS, Satpathy M, Sawhney M, Scarborough P, Schneider IJ, Schöttker B, Schumacher AE, Schwebel DC, Scott JG, Seedat S, Sepanlou SG, Serina PT, Servan-Mori EE, Shackelford KA, Shaheen A, Shahraz S, Shamah Levy T, Shangguan S, She J, Sheikhbahaei S, Shi P, Shibuya K, Shinohara Y, Shiri R, Shishani K, Shiue I, Shrime MG, Sigfusdottir ID, Silberberg DH, Simard EP, Sindi S, Singh A, Singh JA, Singh L, Skirbekk V, Slepak EL, Sliwa K, Soneji S, Søreide K, Soshnikov S, Sposato LA, Sreeramareddy CT, Stanaway JD, Stathopoulou V, Stein DJ, Stein MB, Steiner C, Steiner TJ, Stevens A, Stewart A, Stovner LJ, Stroumpoulis K, Sunguya BF, Swaminathan S, Swaroop M, Sykes BL, Tabb KM, Takahashi K, Tandon N, Tanne D, Tanner M, Tavakkoli M, Taylor HR, Te Ao BJ, Tediosi F, Temesgen AM, Templin T, Ten Have M, Tenkorang EY, Terkawi AS, Thomson B, Thorne-Lyman AL, Thrift AG, Thurston GD, Tillmann T, Tonelli M, Topouzis F, Toyoshima H, Traebert J, Tran BX, Trillini M, Truelsen T, Tsilimbaris M, Tuzcu EM, Uchendu US, Ukwaja KN, Undurraga EA, Uzun SB, Van Brakel WH, Van De Vijver S, van Gool CH, Van Os J, Vasankari TJ, Venketasubramanian N, Violante FS, Vlassov VV, Vollset SE, Wagner GR, Wagner J, Waller SG, Wan X, Wang H, Wang J, Wang L, Warouw TS, Weichenthal S, Weiderpass E, Weintraub RG, Wenzhi W, Werdecker A, Westerman R, Whiteford HA, Wilkinson JD, Williams TN, Wolfe CD, Wolock TM, Woolf AD, Wulf S, Wurtz B, Xu G, Yan LL, Yano Y, Ye P, Yentür GK, Yip P, Yonemoto N, Yoon SJ, Younis MZ, Yu C, Zaki ME, Zhao Y, Zheng Y, Zonies D, Zou X, Salomon JA, Lopez AD, Vos T (2015) Global, regional, and national disability-adjusted life years (DALYs) for 306 diseases and injuries and healthy life expectancy (HALE) for 188 countries, 1990-2013: quantifying the epidemiological transition. Lancet **386**: 2145-2191.

Naqvi SM, Buckley CT (2015) Extracellular matrix production by nucleus pulposus and bone marrow

stem cells in response to altered oxygen and glucose microenvironments. J Anat **227**: 757-766.

Neidlinger-Wilke C, Mietsch A, Rinkler C, Wilke HJ, Ignatius A, Urban J (2012) Interactions of environmental conditions and mechanical loads have influence on matrix turnover by nucleus pulposus cells. J Orthop Res **30**: 112-121.

Noriega DC, Ardura F, Hernández-Ramajo R, Martín-Ferrero M, Sánchez-Lite I, Toribio B, Alberca M, García V, Moraleda JM, Sánchez A, García-Sancho J (2017) Intervertebral disc repair by allogeneic mesenchymal bone marrow cells: a randomized controlled trial. Transplantation **101**: 1945-1951.

Noris M, Remuzzi G (2013) Overview of complement activation and regulation. Semin Nephrol **33**: 479-492.

Orozco L, Soler R, Morera C, Alberca M, Sánchez A, García-Sancho J (2011) Intervertebral disc repair by autologous mesenchymal bone marrow cells: a pilot study. Transplantation **92**: 822-828.

Parekkadan B, van Poll D, Suganuma K, Carter EA, Berthiaume F, Tilles AW, Yarmush ML (2007) Mesenchymal stem cell-derived molecules reverse fulminant hepatic failure. PLoS One **2**: e941. DOI: 10.1371/journal.pone.0000941.

Pereira CL, Teixeira GQ, Ribeiro-Machado C, Caldeira J, Costa M, Figueiredo F, Fernandes R, Aguiar P, Grad S, Barbosa MA, Gonçalves RM (2016) Mesenchymal stem/stromal cells seeded on cartilaginous endplates promote intervertebral disc regeneration through extracellular matrix remodeling. Sci Rep **6**: 33836. DOI: 10.1038/srep33836.

Pettine K, Suzuki R, Sand T, Murphy M (2016) Treatment of discogenic back pain with autologous bone marrow concentrate injection with minimum two year follow-up. Int Orthop **40**: 135-140.

Pettine KA, Murphy MB, Suzuki RK, Sand TT (2015) Percutaneous injection of autologous bone marrow concentrate cells significantly reduces lumbar discogenic pain through 12 months. Stem Cells **33**: 146-156.

Ponnappan RK, Markova DZ, Antonio PJ, Murray HB, Vaccaro AR, Shapiro IM, Anderson DG, Albert TJ, Risbud MV (2011) An organ culture system to model early degenerative changes of the intervertebral disc. Arthritis Res Ther **13**: R171. DOI: 10.1186/ar3494.

Rannou F, Lee TS, Zhou RH, Chin J, Lotz JC, Mayoux-Benhamou MA, Barbet JP, Chevrot A, Shyy JY (2004) Intervertebral disc degeneration: the role of the mitochondrial pathway in annulus fibrosus cell apoptosis induced by overload. Am J Pathol **164**: 915-924.

Ren G, Zhang L, Zhao X, Xu G, Zhang Y, Roberts AI, Zhao RC, Shi Y (2008) Mesenchymal stem cell-mediated immunosuppression occurs *via* concerted action of chemokines and nitric oxide. Cell Stem Cell **2**: 141-150.

Ricklin D, Lambris JD (2013) Complement in immune and inflammatory disorders: pathophysiological mechanisms. J Immunol **190**: 3831-3838.

Risbud MV, Shapiro IM (2014) Role of cytokines in intervertebral disc degeneration: pain and disc content. Nat Rev Rheumatol **10**: 44-56.

Roberts S, Evans H, Trivedi J, Menage J (2006) Histology and pathology of the human intervertebral disc. J Bone Joint Surg Am **88 Suppl 2**: 10-14.

Rosell A, Arai K, Lok J, He T, Guo S, Navarro M, Montaner J, Katusic ZS, Lo EH (2009) Interleukin-1β augments angiogenic responses of murine endothelial progenitor cells *in vitro*. J Cereb Blood Flow Metab **29**: 933-943.

Saggese T, Teixeira GQ, Wade K, Moll L, Ignatius A, Wilke HJ, Goncalves RM, Neidlinger-Wilke C (2019) Georg Schmorl Prize of the German Spine Society (DWG) 2018: Combined inflammatory and mechanical stress weakens the annulus fibrosus: evidences from a loaded bovine AF organ culture. Eur Spine J **28**: 922-933.

Sakai D, Andersson GB (2015) Stem cell therapy for intervertebral disc regeneration: obstacles and solutions. Nat Rev Rheumatol **11**: 243-256.

Sakai D, Grad S (2015) Advancing the cellular and molecular therapy for intervertebral disc disease. Adv Drug Deliv Rev **84**: 159-171.

Sakai D, Nakamura Y, Nakai T, Mishima T, Kato S, Grad S, Alini M, Risbud MV, Chan D, Cheah KS, Yamamura K, Masuda K, Okano H, Ando K, Mochida J (2012) Exhaustion of nucleus pulposus progenitor cells with ageing and degeneration of the intervertebral disc. Nat Commun **3**: 1264. DOI: 10.1038/ncomms2226.

Saparov A, Ogay V, Nurgozhin T, Jumabay M, Chen WC (2016) Preconditioning of human mesenchymal stem cells to enhance their regulation of the immune response. Stem Cells Int **2016**: 3924858. DOI: 10.1155/2016/3924858.

Soland MA, Bego M, Colletti E, Zanjani ED, St Jeor S, Porada CD, Almeida-Porada G (2013) Mesenchymal stem cells engineered to inhibit complement-mediated damage. PLoS One **8**: e60461. DOI: 10.1371/journal.pone.0060461.

Strassburg S, Richardson SM, Freemont AJ, Hoyland JA (2010) Co-culture induces mesenchymal stem cell differentiation and modulation of the degenerate human nucleus pulposus cell phenotype. Regen Med **5**: 701-711.

Teixeira GQ, Boldt A, Nagl I, Pereira CL, Benz K, Wilke HJ, Ignatius A, Barbosa MA, Goncalves RM, Neidlinger-Wilke C (2016) A degenerative/proinflammatory intervertebral disc organ culture: an *ex vivo* model for anti-inflammatory drug and cell therapy. Tissue Eng Part C Methods **22**: 8-19.

Teixeira GQ, Pereira CL, Ferreira JR, Maia AF, Gomez-Lazaro M, Barbosa MA, Neidlinger-Wilke C, Goncalves RM (2018) Immunomodulation of human mesenchymal stem/stromal cells in intervertebral disc degeneration: insights from a proinflammatory/degenerative *ex vivo* model. Spine (Phila Pa 1976) **43**: E673-E682.

Tu Z, Li Q, Bu H, Lin F (2010) Mesenchymal stem cells inhibit complement activation by secreting factor H. Stem Cells Dev **19**: 1803-1809.

Urban JP (2002) The role of the physicochemical environment in determining disc cell behaviour. Biochem Soc Trans **30**: 858-864.

van Buul GM, Villafuertes E, Bos PK, Waarsing JH, Kops N, Narcisi R, Weinans H, Verhaar JA, Bernsen MR, van Osch GJ (2012) Mesenchymal stem cells secrete factors that inhibit inflammatory processes in short-term osteoarthritic synovium and cartilage explant culture. Osteoarthritis Cartilage **20**: 1186-1196.

van Koppen A, Joles JA, van Balkom BW, Lim SK, de Kleijn D, Giles RH, Verhaar MC (2012) Human embryonic mesenchymal stem cell-derived conditioned medium rescues kidney function in rats with established chronic kidney disease. PLoS One **7**: e38746. DOI: 10.1371/journal.pone.0038746.

Vergroesen PP, Kingma I, Emanuel KS, Hoogendoorn RJ, Welting TJ, van Royen BJ, van Dieën JH, Smit TH (2015) Mechanics and biology in intervertebral disc degeneration: a vicious circle. Osteoarthritis Cartilage **23**: 1057-1070.

Wang Q, Rozelle AL, Lepus CM, Scanzello CR, Song JJ, Larsen DM, Crish JF, Bebek G, Ritter SY, Lindstrom TM, Hwang I, Wong HH, Punzi L, Encarnacion A, Shamloo M, Goodman SB, Wyss-Coray T, Goldring SR, Banda NK, Thurman JM, Gobezie R, Crow MK, Holers VM, Lee DM, Robinson WH (2011) Identification of a central role for complement in osteoarthritis. Nat Med **17**: 1674-1679.

Yoshikawa T, Ueda Y, Miyazaki K, Koizumi M, Takakura Y (2010) Disc regeneration therapy using marrow mesenchymal cell transplantation: a report of two case studies. Spine (Phila Pa 1976) **35**: E475-480.

Yu J, Schollum ML, Wade KR, Broom ND, Urban JP (2015) ISSLS prize winner: a detailed examination of the elastic network leads to a new understanding of annulus fibrosus organization. Spine (Phila Pa 1976) **40**: 1149-1157.

Discussion with Reviewers

Reviewer 1: Is there not a control missing, *i.d.* treatment with MSC secretome without priming?
Authors: In the present study, we did not focus on the treatment of AF tissues with MSC secretome without priming because we have previously demonstrated that priming with IL-1β strongly affects the MSC secretome, significantly increasing the production of proinflammatory mediators IL-6, IL-8, MCP-1, CCL5/RANTES and PGE$_2$ (Ferreira *et al.*, 2021). This study also showed that the secretome produced by primed MSCs downregulates bovine IVD gene expression of proinflammatory cytokines IL-6 and IL-8 and matrix degrading enzyme MMP-1, while MMP-3 and TIMP-2 are upregulated after 48 h of treatment. Moreover,

literature data have shown that MSC priming improves their paracrine immunomodulatory effect and capacity to improve tissue repair/regeneration across the wide range of tissues and pathological conditions, including articular cartilage and IVD degeneration (Ferreira *et al.*, 2018). Therefore, we opted to further investigate the effect of the primed MSC secretome on the proinflammatory/degenerative AF-OC model.

Reviewer 2: If there were no significant changes in the annular delamination strength test following CTS + secretome treatment when compared to controls, how does this contribute to further disc degeneration?

Authors: The MSC secretome modulated the proinflammatory response of AF cells but also influenced the AF collagen content and mechanical properties of the AF tissue stimulated by CTS + IL-1β conditions (Fig. 8). Although no differences were found between the secretome-treated group and the control group regarding peeling strength, less collagen was detected at the protein level (Fig. 4**c**). Therefore, we hypothesised that the decreased collagen content may be a hint for a weakening of the AF mechanical properties. Nevertheless, the peel-force test measures the strength required (at a constant velocity) for the detachment of adjacent AF lamellae through the TLBN, mostly composed of elastin and fibrillin. Therefore, changes in collagen content may not influence the test. Given this, further investigations of the effect of MSC secretome on matrix turnover and disc degeneration will be necessary.

Editor's note: The Scientific Editor responsible for this paper was Sibylle Grad.